Published in final edited form as:
Cell. 2009 November 13; 139(4): 719–730. doi:10.1016/j.cell.2009.10.015.

Concerted Loading of Mcm2-7 Double Hexamers Around DNA during DNA Replication Origin Licensing

Dirk Remus[1], **Fabienne Beuron**[2], **Gökhan Tolun**[3], **Jack D. Griffith**[3], **Edward P. Morris**[2], and **John F.X. Diffley**[1]

[1]Cancer Research UK London Research Institute, Clare Hall Laboratories, South Mimms, EN6 3LD, UK

[2]Section of Structural Biology, The Institute of Cancer Research, London SW3 6JB, UK

[3]Lineberger Comprehensive Cancer Center, University of North Carolina, Chapel Hill, North Carolina 27599, USA

Abstract

The licensing of eukaryotic DNA replication origins, which ensures once per cell cycle replication, involves the loading of six related minichromosome maintenance proteins (Mcm2-7) into prereplicative complexes (pre-RCs). Mcm2-7 forms the core of the replicative DNA helicase, which is inactive in the pre-RC. The ATP-dependent Mcm2-7 loading reaction requires the Origin Recognition Complex (ORC), Cdc6 and Cdt1. We have reconstituted Mcm2-7 loading with purified budding yeast proteins. Using biochemical approaches and electron microscopy, we show that single heptamers of Cdt1·Mcm2-7 are loaded cooperatively into stable, head-to-head Mcm2-7 double hexamers connected via N-terminal rings. DNA runs through a central channel in the double hexamer, and, once loaded, Mcm2-7 can slide passively along double-stranded DNA. Our work has significant implications for understanding how eukaryotic DNA replication origins are chosen and licensed, how replisomes assemble during initiation and how unwinding occurs during DNA replication.

Introduction

In eukaryotic cells, DNA replication initiates from multiple replication origins distributed along multiple chromosomes. This allows cells to replicate large genomes in relatively short periods of time. However, origin usage must be carefully coordinated to ensure the genome is completely replicated in each cell cycle, but no region of the genome is replicated more than once. A two-step mechanism underpins once per cell cycle replication in eukaryotes (Bell and Dutta, 2002; Blow and Dutta, 2005; Diffley, 2004). In the first step, known as licensing, the six subunit Origin Recognition Complex (ORC) together with Cdc6 and Cdt1 load Mcm2-7 onto DNA in a reaction requiring ATP hydrolysis. Mcm2-7, comprising six related polypeptides, is believed to be the engine of the replicative helicase but is inactive in this prereplicative complex (pre-RC). The loading of Mcm2-7 can only occur during G1 phase when cyclin dependent kinase (CDK) activity is low and the anaphase promoting complex/cyclosome (APC/C) is active. In budding yeast, CDKs prevent Mcm2-7 loading by directly phosphorylating and inhibiting each pre-RC component. Pre-RCs are activated in S phase by the combined action of two protein kinases, CDK and the Dbf4-dependent protein kinase

(DDK) comprising a heterodimer of Dbf4 and Cdc7. CDKs work by phosphorylating Sld2 and Sld3, which generates binding sites for tandem pairs of BRCT repeats in Dpb11 (Tanaka et al., 2007; Zegerman and Diffley, 2007), whilst DDK phosphorylates Mcm2-7 directly (Sheu and Stillman, 2006). These events together lead to the loading of Cdc45 and the GINS complex into a pre-initiation complex (pre-IC), which is required for the activation of the Mcm2-7 helicase.

Although we know the order in which initiation factors are recruited to origins, relatively little is known about the biochemical mechanism of pre-RC and pre-IC assembly and how this leads to origin unwinding and replisome assembly. To understand these mechanisms in detail, it will be necessary to reconstitute these reactions with purified proteins.

Results

Purification of pre-RC proteins

We set out to purify pre-RC components for reconstitution experiments. Where possible, proteins were expressed and purified from budding yeast cells arrested in G1 phase, a period of competence for pre-RC assembly *in vivo* (Piatti et al., 1996) and *in vitro* (Seki and Diffley, 2000). ORC was purified from G1 phase cell extracts from a yeast strain that over-expressed all six ORC subunits (Bowers et al., 2004) (Figure 1A and Supplementary Figure 1A). Because Cdc6 protein is highly unstable during G1 phase in budding yeast (Drury et al., 2000), it was expressed in insect cells from a baculovirus vector and purified as an apparent monomer (Figure 1B and Supplementary Figure 1C). The purified Cdc6 migrated in SDS-PAGE as a phosphatase-sensitive doublet (Figure 1C lanes 1,2) indicating that it is phosphorylated. We, therefore, also expressed and purified a mutant Cdc6 lacking all eight CDK phosphorylation sites (Figure 1C lanes 3,4). This protein migrated as a fast-migrating single band in the presence and absence of lambda phosphatase.

To purify Mcm2-7, the Mcm4 subunit was tagged at its C-terminus with a 3XFLAG epitope and purified from the soluble (non-chromatin-bound) fraction of G1 phase yeast extracts by α-FLAG immuno-affinity chromatography followed by Superdex 200 gel-filtration chromatography. Approximately half of the Mcm4 eluted from the Superdex 200 column in a high molecular weight complex that co-fractionated with a series of other polypeptides (Figure 1D). Immunoblot (Figure 1E) and mass-spectrometric analysis (data not shown) identified the co-eluting polypeptides in the complex as Mcm2, Mcm3, Mcm5, Mcm6, Mcm7, and Cdt1. The Cdt1·Mcm2-7 complex eluted in the same fraction as thyroglobulin (670kDa) (Figure 1D), consistent with the predicted molecular weight of a Cdt1·Mcm2-7 heptamer (676kDa). The existence of a stoichiometric complex between Cdt1 and Mcm2-7 is consistent with earlier biochemical and genetic analysis (Kawasaki et al., 2006; Tanaka and Diffley, 2002).

Transmission electron microscopy of negatively-stained, purified Cdt1·Mcm2-7 revealed a relatively homogeneous distribution of globular particles, approximately 15 nm in diameter (Figure 1F). Reference-free classification of ~10,000 particles yielded views that we interpret broadly as top/bottom and side views (Figure 1F). The round top/bottom views feature a central hole or cavity. Presumptive side views feature two distinct, parallel layers of protein density (Figure 1F, white arrows in bottom average panel) separated by a gap and connected by thin protein bridges. These are similar to views of the homohexameric complex of the archaeal Mcm from *Methanothermobacter thermautotrophicus* which assembles from a single Mcm subunit (MthMcm) (Pape et al., 2003). Extra protein density located on the side of the particles and not found in the archaeal complex (arrowheads, Figure 1F) may be due to the non-Mcm Cdt1 subunit. We are currently analysing these images to determine the 3D structure of Cdt1·Mcm2-7. We conclude from EM images and gel filtration results that Cdt1 and Mcm2-7

form a hetero-heptameric complex. Significantly for the work described herein, double heptamers were never seen.

Reconstitution of Mcm2-7 loading

To begin to examine pre-RC assembly *in vitro*, we analysed the recruitment of these purified proteins to linear, origin-containing DNA fragments (1kb) coupled to paramagnetic beads (DNA beads). Figure 2A (lanes 1-3) shows that, after incubation with purified proteins in reactions containing ATP, these DNA beads (but not beads lacking DNA – data not shown) bind ORC, Cdc6, Cdt1 and Mcm subunits. Mcm2-7 loading *in vivo* and in extracts has previously been defined by the generation of Mcm2-7 complexes that remain bound to DNA even after high salt treatment (Bowers et al., 2004; Donovan et al., 1997). Figure 2A (lanes 4-6) shows that high salt (0.5M NaCl) extraction of DNA beads from reactions containing ATP quantitatively removed ORC but not the Mcm subunits. Mcm2-7 loading is distinguished from simple recruitment because loading requires ATP hydrolysis by ORC and Cdc6 (Bowers et al., 2004; Klemm and Bell, 2001; Perkins and Diffley, 1998; Randell et al., 2006; Seki and Diffley, 2000; Weinreich et al., 1999). When ATP-hydrolysis was prevented by incubation with the ATP analogue ATPγS (Figure 2A, lanes 7-12), ORC, Cdc6, Cdt1 and Mcm subunits were all bound to DNA beads after a low salt wash; however, the Mcm subunits along with ORC and Cdt1 were all quantitatively removed from DNA beads by high salt extraction. Figure 2B shows that all six Mcm2-7 subunits are loaded onto DNA in a salt-resistant manner in the presence of ATP, but in the presence of ATPγS, all six Mcm subunits are removed by high salt extraction, suggesting that Mcm2-7 subunits remain associated in one complex during recruitment and after loading onto DNA. From these observations we conclude that a salt-resistant, DNA-bound Mcm2-7 complex is generated upon co-incubation of DNA with purified ORC, Cdc6, and Cdt1·Mcm2-7 in a reaction that requires ATP hydrolysis. Together, these results show that ORC, Cdc6 and Cdt1 are sufficient to perform Mcm2-7 loading *in vitro*, consistent with previous work (Gillespie et al., 2001; Kawasaki et al., 2006).

After high salt wash of the ATP-containing reactions, Cdc6 and Cdt1, along with Mcm2-7, remained associated with the beads (Figure 2A and B), To determine whether these proteins are actually bound to DNA, we treated the salt-washed beads with EcoR1, which cleaves the DNA at a site near the biotin-streptavidin linkage. Figure 2C shows that Cdc6 and Cdt1 remained bound to beads after removal of >95% of the DNA with EcoR1. Mcm2-7, however, were quantitatively removed from beads with the DNA. Thus, retention of Cdc6 and Cdt1 on DNA beads is due to non-specific interactions with the beads after Mcm2-7 loading. By contrast, Mcm2-7 proteins appear to be loaded directly on DNA. Maximum levels of Mcm2-7 loaded onto DNA were reached between 25-40 minutes of incubation (Figure 2D), similar to reported results in extracts (Bowers et al., 2004).

To further examine Mcm2-7 loading, DNA bead-bound proteins were visualised by silver staining after SDS-PAGE. Figure 2E shows that very similar amounts of Mcm2-7 and ORC were loaded onto DNA during the course of the reaction (lanes 2-4). In separate experiments, up to 20% of the input Mcm2-7 was converted into salt-resistant DNA-bound complexes (data not shown). We conclude that the Mcm2-7 loading reaction with purified proteins is relatively efficient, unlike the loading of Mcm2-7 in cell extracts (Seki and Diffley, 2000).

ORC and Cdc6 act together to recruit and load Mcm2-7

Figure 3A shows that Mcm2-7 subunits were neither recruited nor loaded onto DNA in the absence of Cdc6 protein (lanes 1, 5, 9, 13) indicating that ORC alone cannot efficiently recruit Cdt1·Mcm2-7. Similarly, Mcm2-7 subunits were neither recruited nor loaded in the absence of ORC (Figure 3B, lanes 1, 5, 9, 13). In both Figure 3A and 3B, ATP-dependent Mcm2-7

loading was rescued by titrating the missing component back into these reactions. These experiments show that ORC and Cdc6 are both required to recruit Cdt1·Mcm2-7 to DNA.

As shown in Figure 1C, the Cdc6 protein used here is at least partly phosphorylated, presumably by endogenous insect cell CDKs. Figure 3C shows, however, loading efficiencies of Cdc6-wt were indistinguishable from those of Cdc6-8A across a range of concentrations. Therefore, CDK phosphorylation of Cdc6 does not directly inhibit Mcm2-7 loading in this system, consistent with previous work showing that CDK inhibition of Cdc6 function requires additional protein co-factors, including SCF^{CDC4} and Clb2-Cdc28 (Drury et al., 2000; Mimura et al., 2004).

Role of DNA sequence in Mcm2-7 loading

The initiation of DNA replication in budding yeast, unlike metazoans, depends on specific DNA sequences. These origins serve as specific binding sites for ORC and are also the sites at which pre-RCs assemble. The A element of the well-characterised ARS1 contains the essential ARS consensus sequence (ACS), which, together with the non-essential B1 element, defines the primary ORC binding site (Bell and Stillman, 1992; Marahrens and Stillman, 1992; Rao and Stillman, 1995; Rowley et al., 1995). The B2 element contains a 9/11 match to the ACS and can bind ORC in the absence of the ACS (Bell and Stillman, 1992). We therefore compared ORC binding and Mcm2-7 loading on wild type ARS1 and a $A^{-}B2^{-}$ double mutant, which removes all known ORC binding sites. Surprisingly, Figure 3D shows that, in the absence of competitor DNA, ORC is recruited equally well, even at sub-stoichiometric concentrations, to the wild type ARS1 and the $A^{-}B2^{-}$ double mutant (Figure 3D, lanes 1,2,5,6). Figure 3D also shows that Mcm2-7 loading efficiency was indistinguishable between wild type and the $A^{-}B2^{-}$ mutant ARS1 in the absence of competitor DNA (lanes 1-8). Addition of non-specific competitor DNA strongly suppressed the binding of ORC as well as Mcm2-7 to both wild type and $A^{-}B2^{-}$ mutant DNA (data not shown), and, under these conditions, ORC specifically associated with the wild-type ARS1 DNA (Figure 3D, compare lanes 9-10 and 13-14). Mcm2-7 loading was also preferentially observed on wild-type origin DNA in these reactions (Figure 3D, lanes 9-16). These data suggest that purified ORC, Cdc6, and Cdt1·Mcm2-7 can mediate sequence-specific Mcm2-7 loading *in vitro* in the presence of competitor DNA, yet specific sequences are not mechanistically required for either ORC binding or Mcm2-7 loading.

Mcm2-7 are loaded as double hexamers

As shown in Figure 2C (lane 4), the loaded Mcm2-7 complexes can be purified after high salt wash by removal of the DNA from beads with EcoR1. Upon examination by EM after negative staining, the majority of the Mcm2-7 particles present in this fraction were roughly rectangular and homogeneous in size (150 Å × 230 Å)(Figure 4A and Supplementary Figure 4A,B). Image analysis and classification of individual particles showed them to be composed of four parallel layers of protein density (Figure 4C, upper panel), with the two outer layers being thicker than the two inner layers. Protein density was reduced along the long axis through the center of the particles, suggesting that a channel runs through the particle. The height of this four layer Mcm2-7 complex is roughly twice that of the two-layer Cdt1·Mcm2-7 complex. Thus, the loaded complex appears to be a double hexamer of Mcm2-7.

To test whether the double hexamer was the result of enforced hydrophobic interactions induced by exposure to high-salt, we omitted the high-salt wash and analyzed the entire loading reaction in solution rather than on beads. Reactions were incubated with free 1 kb DNA fragments and spotted directly onto carbon-coated copper grids for electron-microscopic analysis. As shown in the overview image of Figure 4B, the same rectangular double-hexameric particles were readily seen against a background of smaller, more heterogeneous complexes

that likely correspond to free Cdt1·Mcm2-7 complexes and ORC. Image analysis confirmed that these abundant, larger particles were structurally indistinguishable from the Mcm2-7 particles purified after high salt wash (Figure 4C, lower panel). Double hexamers were not detected in reactions that lacked either DNA, ORC, or Cdc6. They were also not detected in complete reactions that were performed in the presence of ATPγS (Supplementary Figure 2).

These double hexamers are similar to 2D class averages of electron-microscopic images of double-hexameric assemblies of the archaeal MthMcm (Costa et al., 2006). In the case of MthMcm, molecular modelling indicated that the thicker outer tiers of the double-hexamer contain the AAA+ domains, whereas the two inner tiers correspond to the double-hexameric ring of the N-terminal domain that mediates hexamer-hexamer association. The Mcm2-7 double hexamer appears to have a similar organisation. To obtain independent evidence of the orientation of the individual hexamers, we took advantage of the FLAG epitope tag on the Mcm4 C-terminus. We performed loading as in Figure 4A except reactions contained purified α-FLAG antibody. Figure 4D shows that the extra density resulting from the antibody-labelling of the Mcm4 C-terminus was specifically associated with the outer tiers of the structure and the sites of antibody attachment on either end of the double-hexamers appeared to be spatially related by rotational symmetry. Terminally bound IgG was also observed in cases where only one IgG was bound to an Mcm2-7 double hexamer or where one IgG was simultaneously bound to two Mcm2-7 double hexamers (Supplementary Figure 3). Thus, Mcm2-7 are loaded as head-to-head double hexamers with the C-terminal AAA+ domain located in the thicker tiers on the outside of the double hexamer.

A three-dimensional model of the Mcm2-7 double hexamer

We calculated a 3D reconstruction of the Mcm2-7 double hexamer to ~30 Å resolution from 2292 particles out of a 3700 particles dataset (Supplementary Figure 4). Surface representations of a series of angular rotations around the long axis of the particles and an end-on view are shown in Figure 5A-E. The overall barrel-like structure (150 Å × 230 Å) exhibits four ring-like tiers of protein density consistent with the density described for the 2D class averages above. 2D reprojections of the 3D model agree well with the 2D class averages, supporting the validity of the 3D map (Supplementary Figure 4B). The two hexamers are connected by multiple thin protein bridges at the inner and outer circumference of the N-terminal rings (Figure 5 and Supplementary Figure 4F). This differs slightly from the X-ray structure of the double hexameric MthMcm N-terminal ring, which is connected primarily by interactions near the inner circumference of the N-terminal rings (Fletcher et al., 2003). Several eukaryotic Mcms (2,4,6) have extended N-terminal domains not found in Archaea, which may contribute to these inter-hexamer interactions. Similar to the MthMcm hexamer, side openings are found between the N-terminal and AAA+ rings in each hexamer (Figure 5A-D). The end-on view (Figure 5E), the cut-away view (Figure 5F), and the density sections (Supplementary Figure 4C) show that a central channel runs through the entire length of the double hexamer. Both the cut-away view of the surface-rendered 3D model and serial density sections through the double-hexameric structure reveal that the channel bends at the interface between the two hexameric halves due to off-register stacking of the hexamers (Figure 5F and Supplementary Figure 4C).

Mobility of Mcm2-7 double hexamers on DNA

The presence of the central channel suggests a path for DNA through the Mcm2-7 double hexamer, although DNA density was not directly recovered in the 3D reconstruction. We used direct mounting and tungsten rotary shadowing of purified, loaded Mcm2-7 complexes to visualize the DNA associated with Mcm2-7 double hexamers. Mcm2-7 particles bound to linear 1kb DNA fragments (Figure 6A) exhibited similar shape and dimension (166 ± 15 Å × 249 ± 13 Å [n = 75]) to the Mcm2-7 double hexamer described above. The small increase in overall dimensions of the double hexamer is likely due to deposition of tungsten. Very few

DNA molecules contained more than one double hexamer. In specimens where we could unambiguously trace the contour of the DNA molecules, the DNA appeared to enter and exit from opposite ends of the Mcm2-7 double hexamer (Figure 6A). In addition, free DNA molecules exhibited mean DNA contour lengths that were not significantly different from those bound by Mcm2-7 double hexamers (318 nm ± 16 nm [n=30] versus 321 nm ± 31 nm [n=43], respectively). These observations are consistent with DNA passing through the central channel of Mcm2-7 double hexamers. We do not exclude the possibility that Mcm2-7 may also engage DNA by other mechanisms (Costa et al., 2008).

If DNA passed through this central channel, Mcm2-7 would be topologically linked to the DNA. To test this, we asked whether circularisation of the bound DNA prevented dissociation of Mcm2-7. Figure 6B shows that Mcm2-7 exhibited a half-life on DNA of only approximately 10 minutes on 1 kb linear DNA in high-salt (0.5M NaCl) buffer (Figure 6B). This could reflect the overall instability of the complex, or it could reflect the loss of Mcm2-7 from the ends of these short, linear molecules. To distinguish between these possibilities, we compared residence times of Mcm2-7 double hexamers on a 1 kb linear DNA template to a circularised version of the same 1 kb DNA fragment. Strikingly, Figure 6C shows that Mcm2-7 double hexamers exhibited a half-life on the circular DNA that greatly exceeded 60 minutes, compared to 10 minutes on linear DNA (Figure 6C, lanes 6-10, and graph below). Figure 6C also shows that the loss of Mcm2-7 from the linear DNA occurred at the same rate in the presence or absence of ATP. These data strongly suggest that Mcm2-7 double hexamers can slide off the ends of a linear DNA molecule in an ATP-independent fashion and are therefore topologically linked to the DNA. At a more physiological salt concentration (0.1M NaCl), the half-life of Mcm2-7 double hexamers on linear DNA increased to approximately 35 minutes (Figure 6D, lanes 1-5 and graph below). This longer half-life on linear DNA is presumably due to electrostatic interactions between DNA and Mcm2-7. However, this is still significantly shorter than the half-life of Mcm2-7 double hexamers on the circular DNA template, which was greater than 60 minutes (Figure 6D, lanes 6-10 and graph below). Again, the rate of Mcm2-7 loss was not affected by the presence of ATP. Taken together, these experiments show that Mcm2-7 double hexamers encircle and bind DNA in the central channel, and that once bound to DNA, the double hexamers are mobile.

Because this sliding activity might have led to an underestimate of double hexamer formation by EM, we reinvestigated the binding to circular DNA by EM using rotary shadowing. Most DNA molecules contained either zero or one double hexamer (examples of one double hexamer in Figure 6E, i, ii, iii). Although there were DNA molecules with two or three double hexamers (Figure 6E, iv, v), these accounted for fewer than 5% of the protein:DNA complexes arguing that loading of multiple double hexamers is unlikely to be processive. The appearance of relaxed circular DNA bound to Mcm2-7 is consistent with the idea that the double hexamers do not contain extensive single-stranded DNA.

Discussion

Our results provide the first evidence that ORC and Cdc6 load the Mcm2-7 proteins from single Cdt1·Mcm2-7 heptamers into pre-RCs as head-to-head double hexamers. DNA, probably double stranded, passes through the long, central channel of this double hexamer. And, once loaded, the double hexamer is mobile, capable of passive one-dimensional diffusion or ‘sliding’ along DNA. These features of the pre-RC have implications for how origins are chosen and how replisomes assemble during initiation.

The loading of Mcm2-7 requires ORC, Cdc6 and hydrolysable ATP, consistent with requirements *in vivo*. The requirement for Cdt1 was not tested because it is an integral component of the Mcm2-7 complex. The interaction of Cdt1 with both Mcm2-7 and Orc6

(Chen et al., 2007), suggests that it may act as a bridge between ORC and Mcm2-7. However, our results demonstrate that Cdc6 is also essential to recruit Mcm2-7 to origins, indicating that additional interactions are involved in this recruitment.

Surprisingly, loading of Mcm2-7 *in vitro* does not require specific ORC binding sites. Our results may contribute to resolving the long-standing issue of how orthologues of ORC can act on specific DNA sequences in yeast, but show little or no sequence preference in metazoans (Gilbert, 2004). Our results indicate that even yeast ORC has no inherent mechanistic requirement for specific DNA sequences in the loading of Mcm2-7. The sequence specific DNA binding of the budding yeast ORC may be an evolutionary adaptation designed to ensure sufficient origin activity in a genome containing very little intergenic DNA (Brewer, 1994). Sequence specificity appears to be an integral part of the *S.cerevisiae* core ORC whilst sequence specificity of *Schizosaccharomyces pombe* ORC is conferred by an extended AT hook domain on the Orc4 subunit (Chuang et al., 2002; Kong and DePamphilis, 2001; Lee et al., 2001). Recruitment of ORC in metazoans may also involve interactions with additional sequence specific DNA binding proteins like TRF2 (Atanasiu et al., 2006; Deng et al., 2007; Tatsumi et al., 2008). Consistent with this idea, recruitment of ORC to a GAL4 DNA binding site array via fusion of ORC subunits or Cdc6 to the GAL4 DNA binding domain is sufficient to create a functional replication origin in human cells (Takeda et al., 2005).

In *E.coli*, the ATP-bound DnaA initator binds to 9-mer sequences in *oriC* causing localised DNA unwinding in adjacent 13-mer sequences (Bramhill and Kornberg, 1988). The two DnaB helicase hexamers are then recruited to load around the unwound 13-mer strands by slightly different mechanisms (Mott et al., 2008). Unlike DnaA binding, ORC binding does not induce any detectable DNA unwinding. Thus, the eukaryotic initiator does not generate single-stranded DNA for the Mcm2-7 helicase to encircle. Moreover, previous analysis of yeast origins *in vivo* failed to detect any $KMnO_4$-reactive DNA in G1-arrested cells (Geraghty et al., 2000) and data not shown) indicating that initial origin melting does not occur when Mcm2-7 is loaded onto DNA but, instead, occurs when the helicase is activated during S phase. Consistent with this, the ability of loaded Mcm2-7 to slide freely on double-stranded DNA in an ATP-independent manner (Figure 6B-D) indicates that Mcm2-7 loaded *in vitro* encircles double-stranded, not single-stranded DNA. Delaying the generation of single stranded DNA within the Mcm2-7 double hexamer until S phase may protect origin DNA from damage during G1 phase.

The loading of the double hexamer appears to be highly cooperative. Double Cdt1·Mcm2-7 heptamers were never seen prior to loading and single Mcm2-7 hexamers were never detected on DNA after loading. These results indicate that the two hexamers are loaded together in a concerted reaction. The stoichiometry of ORC and Cdc6 in this loading reaction is presently unknown. Although yeast origins generally contain a single high affinity ORC binding site, a second potential ORC binding site resides within the B2 element of ARS1 (Wilmes and Bell, 2002). Additionally, archaeal replication origins, which may initiate replication by mechanisms similar to eukaryotes, generally have ORC binding sites arranged symmetrically around an A/T rich region (Wigley, 2009). The lack of stringent sequence requirement suggests that a second ORC binding site need not be a specific sequence element. We note that this concerted loading reaction requires the coordinated breaking and reforming of four separate rings, two in each hexamer. Further work will be required to elucidate the mechanism of this complex loading reaction and to determine the functionality of the loaded Mcm2-7 double hexamer.

The binding of Mcm2-7 around double stranded DNA has implications for how DNA unwinding is ultimately catalysed by the Cdc45/Mcm2-7/GINS (CMG) complex (Moyer et al., 2006). Mcm2-7 may act in unwinding analogously to the eukaryotic viral SF3 initiator/helicases including the SV40 large T antigen (TAg) and the papillomavirus E1 protein. The

TAg double hexamer can bind to double stranded DNA, and this binding can induce the generation of a short (8bp) stretch of melted DNA specifically within one of the two hexamers (Borowiec and Hurwitz, 1988). Although TAg and E1 can assemble as double hexamers around double stranded DNA (Dean et al., 1992; Fouts et al., 1999; Liu et al., 1998), current models indicate that they act during unwinding as classical helicases by encircling single stranded DNA (Enemark and Joshua-Tor, 2008; Schuck and Stenlund, 2005). If Mcm2-7 act analogously to these proteins, CDK- and DDK-dependent events must promote remodelling of the Mcm2-7 complex to encircle single stranded DNA during origin melting.

Alternatively, Mcm2-7 may act during replication as a double-strand DNA translocase (Laskey and Madine, 2003). In this model, Cdc45 and/or GINS would play a direct, structural role in strand separation, perhaps acting as a 'plough' or 'pin' into which DNA is pumped by Mcm2-7 (Takahashi et al., 2005). This is analogous to the bacterial RuvAB Holliday junction branch migrating enzyme in which two RuvB hexamers pump double stranded DNA through a tetramer of RuvA, which coordinates the separation and re-annealing of strands (West, 2003). We currently favour this second model because it does not require topological reorganisation of Mcm2-7 subunits during initiation and because it provides a potential biochemical function for Cdc45 and/or GINS during replication. The helicase activity of archaeal Mcm (Chong et al., 2000; Kelman et al., 1999; Shechter et al., 2000) as well as eukaryotic Mcm complexes (Bochman and Schwacha, 2008; Ishimi, 1997; Moyer et al., 2006) on ssDNA substrates need not reflect their mode of action *in vivo*: even double stranded DNA translocases like RuvB can function in standard helicase assays (Tsaneva et al., 1993), presumably because they can translocate along one strand of DNA and displace annealed oligonucleotides.

By analogy to the mode of action of both SV40 large T antigen and RuvB, the orientation of the Mcm2-7 hexamers suggests that DNA is translocated from the AAA+ domains towards the N-terminal domains in each hexamer (Li et al., 2003; VanLoock et al., 2002; Wessel et al., 1992; West, 2003). Consistent with this, the archaeal MCM hexamer from *Sulfolobus solfataricus* (SsoMCM) can be loaded onto the 3' single-stranded overhang of a forked substrate, with its AAA+ domain facing the fork (McGeoch et al., 2005).

The purified Replisome Progression Complex (RPC), a protein assemblage containing the CMG complex as well as other replisome components, contains just a single copy of Mcm4 (and presumably the other Mcm2-7 subunits) (Gambus et al., 2006). Thus, the functional unit of Mcm2-7 in elongation may be the single hexamer. We note that DDK, required for helicase activation, acts on N-terminal tails of Mcm2, 4 and 6 (Sheu and Stillman, 2006). Moreover, the *mcm5-bob1* allele, which bypasses the requirement for DDK, is a mutation in the N-terminal domain of Mcm5 near the interface between hexamers (Fletcher et al., 2003). We speculate that DDK may activate the helicase by inducing separation of the two hexamers and the *mcm5-bob1* allele may mimic this by destabilising interactions between hexamers.

The length of an Mcm2-7 double hexamer (230 Å) corresponds to approximately 68bp of B form DNA. This is similar to the size of the pre-RC footprint at several origins *in vivo* (Diffley et al., 1994; Santocanale and Diffley, 1996). However, based on data from Donovan et al. (1997), the equivalent of approximately 5 double hexamers are loaded per origin in yeast. The pre-RC footprint cannot account for this number of double hexamers. Indeed, the loading of multiple Mcm2-7 complexes per origin appears to be a common feature in eukaryotes (Hyrien et al., 2003). Once loaded, Mcm2-7 double hexamers may slide away from origins, allowing repeated loading. Although multiple Mcm2-7 complexes are loaded per origin, there is currently no evidence that this loading is processive and our results indicate that loading *in vitro* is distributive. Additional activities would presumably be required to allow the double hexamers to slide past nucleosomes bordering origins. Since ORC and Cdc6 can promote

sequence-independent loading of Mcm2-7 (Figure 3D), it is also possible that some Mcm2-7 is loaded outside of origins, perhaps at random locations *in vivo*, which might not have been detectable in ChIP-chip experiments (Wyrick et al., 2001). These extra Mcm2-7 complexes may act as 'spare' origins to rescue stalled replication forks (Ge et al., 2007; Woodward et al., 2006).

The ability of the double hexamer to slide on double stranded DNA provides a mechanism by which supernumerary Mcm2-7 double hexamers may be pushed ahead of the replisome during normal elongation. These excess double hexamers could play a role in restoring an active helicase at stalled forks. This might provide an important mechanism for replication restart that does not require the reloading of soluble Mcm2-7 and, therefore, does not compromise mechanisms designed to ensure once per cell cycle replication.

Experimental procedures

Proteins

Expression and purification protocols are included as supplementary data.

DNA templates

Linear DNAs containing ARS1 or ARS305 were generated by PCR as described in supplementary methods. Circular ARS305-containing DNA was prepared as in (Pacek et al., 2006).

Loading reaction

Loading reactions were performed in 40 μl of 25 mM Hepes-KOH pH 7.6/0.1M K-glutamate/0.02% NP-40/10 mM $Mg(OAc)_2$/5% glycerol/1 mM DTT and 5 mM ATP or ATPγS. DNA beads were included at 1 pmol (25 nM) of DNA molecules. Reactions were mixed on ice and incubated at 30°C. Beads were washed once with 0.4 ml low-salt wash buffer (25 mM Hepes-KOH pH 7.6/0.3 M K-glutamate/0.02% NP-40/5 mM $Mg(OAc)_2$/1 mM EDTA/1 mM EGTA/10% glycerol/1 mM DTT) and once with 0.4 ml high-salt wash buffer (as low-salt buffer, but 0.5 M NaCl instead of 0.3 M K-glutamate).

Electron microscopy

Mcm2-7-DNA complexes were purified from a standard loading reaction, followed by cleavage of the DNA in 40 μl of 25 mM Hepes-KOH pH 7.6/0.1 M K-glutamate/0.02% NP-40/5 mM $Mg(OAc)_2$/5% glycerol with EcoR1 for 25 minutes at 30°C. IgG-labelled Mcm2-7 double hexamers were purified similar to unlabelled complexes, except that 1 μmg of a-FLAG M2 antibody (Sigma) was added to a loading reaction 10 minutes before the wash. Sample preparation and image processing were carried out as described in supplementary methods.

For rotary shadowing, Mcm2-7- complexes bound to linear DNA were eluted from beads with EcoR1 in 25 mM Hepes-NaOH pH 7.6/ 50 mM NaCl/5 mM $Mg(OAc)_2$/5% glycerol. Mcm2-7 complexes bound to circularized DNA were purified from loading reactions in solution by gel filtration on Superose 6 in EcoR1 digestion buffer. The sample was prepared as described (Griffith and Christiansen, 1978) with modifications (supplementary methods).

Supplementary Material

Refer to Web version on PubMed Central for supplementary material.

Acknowledgments

This work was funded by Cancer Research UK (DR, JFXD, FB, EPM), ICR (FB and EPM) and NIH grants to JDG (GM31819 and ES13773). DR was supported by an EMBO long term fellowship. We are grateful to Dale Wigley for help and advice in the early stages of this project and to Dr Paula da Fonseca for advice on image processing. We thank Mark Skehel and colleagues for mass spectrometry and Karim Labib for antibodies. We are also grateful to members of the Diffley laboratory for helpful discussions.

References

Atanasiu C, Deng Z, Wiedmer A, Norseen J, Lieberman PM. ORC binding to TRF2 stimulates OriP replication. EMBO Rep 2006;7:716–721. [PubMed: 16799465]

Bell SP, Dutta A. DNA replication in eukaryotic cells. Annu Rev Biochem 2002;71:333–374. [PubMed: 12045100]

Bell SP, Stillman B. ATP-dependent recognition of eukaryotic origins of DNA replication by a multiprotein complex. Nature 1992;357:128–134. [PubMed: 1579162]

Blow JJ, Dutta A. Preventing re-replication of chromosomal DNA. Nat Rev Mol Cell Biol 2005;6:476–486. [PubMed: 15928711]

Bochman ML, Schwacha A. The Mcm2-7 complex has in vitro helicase activity. Mol Cell 2008;31:287–293. [PubMed: 18657510]

Borowiec JA, Hurwitz J. Localized melting and structural changes in the SV40 origin of replication induced by T-antigen. EMBO J 1988;7:3149–3158. [PubMed: 2846276]

Bowers JL, Randell JC, Chen S, Bell SP. ATP hydrolysis by ORC catalyzes reiterative Mcm2-7 assembly at a defined origin of replication. Mol Cell 2004;16:967–978. [PubMed: 15610739]

Bramhill D, Kornberg A. Duplex opening by dnaA protein at novel sequences in initiation of replication at the origin of the E. coli chromosome. Cell 1988;52:743–755. [PubMed: 2830993]

Brewer BJ. Intergenic DNA and the sequence requirements for replication initiation in eukaryotes. Curr Opin Genet Dev 1994;4:196–202. [PubMed: 8032196]

Chen S, de Vries MA, Bell SP. Orc6 is required for dynamic recruitment of Cdt1 during repeated Mcm2-7 loading. Genes Dev 2007;21:2897–2907. [PubMed: 18006685]

Chong JP, Hayashi MK, Simon MN, Xu RM, Stillman B. A double-hexamer archaeal minichromosome maintenance protein is an ATP-dependent DNA helicase. Proc Natl Acad Sci U S A 2000;97:1530–1535. [PubMed: 10677495]

Chuang RY, Chretien L, Dai J, Kelly TJ. Purification and characterization of the Schizosaccharomyces pombe origin recognition complex: interaction with origin DNA and Cdc18 protein. J Biol Chem 2002;277:16920–16927. [PubMed: 11850415]

Costa A, Pape T, van Heel M, Brick P, Patwardhan A, Onesti S. Structural studies of the archaeal MCM complex in different functional states. J Struct Biol 2006;156:210–219. [PubMed: 16731005]

Costa A, van Duinen G, Medagli B, Chong J, Sakakibara N, Kelman Z, Nair SK, Patwardhan A, Onesti S. Cryo-electron microscopy reveals a novel DNA-binding site on the MCM helicase. Embo J 2008;27:2250–2258. [PubMed: 18650940]

Dean FB, Borowiec JA, Eki T, Hurwitz J. The simian virus 40 T antigen double hexamer assembles around the DNA at the replication origin. J Biol Chem 1992;267:14129–14137. [PubMed: 1321135]

Deng Z, Dheekollu J, Broccoli D, Dutta A, Lieberman PM. The origin recognition complex localizes to telomere repeats and prevents telomere-circle formation. Curr Biol 2007;17:1989–1995. [PubMed: 18006317]

Diffley JF. Regulation of early events in chromosome replication. Curr Biol 2004;14:R778–786. [PubMed: 15380092]

Diffley JF, Cocker JH, Dowell SJ, Rowley A. Two steps in the assembly of complexes at yeast replication origins in vivo. Cell 1994;78:303–316. [PubMed: 8044842]

Donovan S, Harwood J, Drury LS, Diffley JF. Cdc6p-dependent loading of Mcm proteins onto pre-replicative chromatin in budding yeast. Proc Natl Acad Sci U S A 1997;94:5611–5616. [PubMed: 9159120]

Drury LS, Perkins G, Diffley JFX. The Cyclin Dependent Kinase Cdc28p Regulates Distinct Modes of Cdc6p Proteolysis during the Budding Yeast Cell Cycle. Curr Biol 2000;10:231–240. [PubMed: 10712901]

Enemark EJ, Joshua-Tor L. On helicases and other motor proteins. Curr Opin Struct Biol 2008;18:243–257. [PubMed: 18329872]

Fletcher RJ, Bishop BE, Leon RP, Sclafani RA, Ogata CM, Chen XS. The structure and function of MCM from archaeal M. Thermoautotrophicum. Nat Struct Biol 2003;10:160–167. [PubMed: 12548282]

Fouts ET, Yu X, Egelman EH, Botchan MR. Biochemical and electron microscopic image analysis of the hexameric E1 helicase. J Biol Chem 1999;274:4447–4458. [PubMed: 9933649]

Gambus A, Jones RC, Sanchez-Diaz A, Kanemaki M, van Deursen F, Edmondson RD, Labib K. GINS maintains association of Cdc45 with MCM in replisome progression complexes at eukaryotic DNA replication forks. Nat Cell Biol 2006;8:358–366. [PubMed: 16531994]

Ge XQ, Jackson DA, Blow JJ. Dormant origins licensed by excess Mcm2-7 are required for human cells to survive replicative stress. Genes Dev 2007;21:3331–3341. [PubMed: 18079179]

Geraghty DS, Ding M, Heintz NH, Pederson DS. Premature structural changes at replication origins in a yeast minichromosome maintenance (MCM) mutant. J Biol Chem 2000;275:18011–18021. [PubMed: 10751424]

Gilbert DM. In search of the holy replicator. Nat Rev Mol Cell Biol 2004;5:848–855. [PubMed: 15459665]

Gillespie PJ, Li A, Blow JJ. Reconstitution of licensed replication origins on *Xenopus* sperm nuclei using purified proteins. BMC Biochem 2001;2:15. [PubMed: 11737877]

Griffith JD, Christiansen G. Electron microscope visualization of chromatin and other DNA-protein complexes. Annu Rev Biophys Bioeng 1978;7:19–35. [PubMed: 78683]

Hyrien O, Marheineke K, Goldar A. Paradoxes of eukaryotic DNA replication: MCM proteins and the random completion problem. Bioessays 2003;25:116–125. [PubMed: 12539237]

Ishimi Y. A DNA helicase activity is associated with an MCM4, -6, and -7 protein complex. J Biol Chem 1997;272:24508–24513. [PubMed: 9305914]

Kawasaki Y, Kim HD, Kojima A, Seki T, Sugino A. Reconstitution of Saccharomyces cerevisiae prereplicative complex assembly in vitro. Genes Cells 2006;11:745–756. [PubMed: 16824194]

Kelman Z, Lee JK, Hurwitz J. The single minichromosome maintenance protein of Methanobacterium thermoautotrophicum DeltaH contains DNA helicase activity. Proc Natl Acad Sci U S A 1999;96:14783–14788. [PubMed: 10611290]

Klemm RD, Bell SP. ATP bound to the origin recognition complex is important for preRC formation. Proc Natl Acad Sci U S A 2001;98:8361–8367. [PubMed: 11459976]

Kong D, DePamphilis ML. Site-specific DNA binding of the Schizosaccharomyces pombe origin recognition complex is determined by the Orc4 subunit. Mol Cell Biol 2001;21:8095–8103. [PubMed: 11689699]

Laskey RA, Madine MA. A rotary pumping model for helicase function of MCM proteins at a distance from replication forks. EMBO Rep 2003;4:26–30. [PubMed: 12524516]

Lee JK, Moon KY, Jiang Y, Hurwitz J. The Schizosaccharomyces pombe origin recognition complex interacts with multiple AT-rich regions of the replication origin DNA by means of the AT-hook domains of the spOrc4 protein. Proc Natl Acad Sci U S A 2001;98:13589–13594. [PubMed: 11717425]

Li D, Zhao R, Lilyestrom W, Gai D, Zhang R, DeCaprio JA, Fanning E, Jochimiak A, Szakonyi G, Chen XS. Structure of the replicative helicase of the oncoprotein SV40 large tumour antigen. Nature 2003;423:512–518. [PubMed: 12774115]

Liu JS, Kuo SR, Makhov AM, Cyr DM, Griffith JD, Broker TR, Chow LT. Human Hsp70 and Hsp40 chaperone proteins facilitate human papillomavirus-11 E1 protein binding to the origin and stimulate cell-free DNA replication. J Biol Chem 1998;273:30704–30712. [PubMed: 9804845]

Marahrens Y, Stillman B. A yeast chromosomal origin of DNA replication defined by multiple functional elements. Science 1992;255:817–823. [PubMed: 1536007]

McGeoch AT, Trakselis MA, Laskey RA, Bell SD. Organization of the archaeal MCM complex on DNA and implications for the helicase mechanism. Nat Struct Mol Biol 2005;12:756–762. [PubMed: 16116441]

Mimura S, Seki T, Tanaka S, Diffley JF. Phosphorylation-dependent binding of mitotic cyclins to Cdc6 contributes to DNA replication control. Nature 2004;431:1118–1123. [PubMed: 15496876]

Mott ML, Erzberger JP, Coons MM, Berger JM. Structural synergy and molecular crosstalk between bacterial helicase loaders and replication initiators. Cell 2008;135:623–634. [PubMed: 19013274]

Moyer SE, Lewis PW, Botchan MR. Isolation of the Cdc45/Mcm2-7/GINS (CMG) complex, a candidate for the eukaryotic DNA replication fork helicase. Proc Natl Acad Sci U S A 2006;103:10236–10241. [PubMed: 16798881]

Pacek M, Tutter AV, Kubota Y, Takisawa H, Walter JC. Localization of Mcm2-7, Cdc45, and GINS to the site of DNA unwinding during eukaryotic DNA replication. Mol Cell 2006;21:581–587. [PubMed: 16483939]

Pape T, Meka H, Chen S, Vicentini G, van Heel M, Onesti S. Hexameric ring structure of the full-length archaeal MCM protein complex. EMBO Rep 2003;4:1079–1083. [PubMed: 14566326]

Perkins G, Diffley JF. Nucleotide-dependent prereplicative complex assembly by Cdc6p, a homolog of eukaryotic and prokaryotic clamp-loaders. Mol Cell 1998;2:23–32. [PubMed: 9702188]

Piatti S, Bohm T, Cocker JH, Diffley JF, Nasmyth K. Activation of S-phase-promoting CDKs in late G1 defines a "point of no return" after which Cdc6 synthesis cannot promote DNA replication in yeast. Genes Dev 1996;10:1516–1531. [PubMed: 8666235]

Randell JC, Bowers JL, Rodriguez HK, Bell SP. Sequential ATP hydrolysis by Cdc6 and ORC directs loading of the Mcm2-7 helicase. Mol Cell 2006;21:29–39. [PubMed: 16387651]

Rao H, Stillman B. The origin recognition complex interacts with a bipartite DNA binding site within yeast replicators. Proc Natl Acad Sci USA 1995;92:2224–2228. [PubMed: 7892251]

Rowley A, Cocker JH, Harwood J, Diffley JFX. Initiation Complex Assembly at Budding Yeast Replication Origins Begins with the Recognition of a Bipartite Sequence by Limiting Amounts of the Initiator, ORC. EMBO J 1995;14:2631–2641. [PubMed: 7781615]

Santocanale C, Diffley JF. ORC- and Cdc6-dependent complexes at active and inactive chromosomal replication origins in Saccharomyces cerevisiae. EMBO J 1996;15:6671–6679. [PubMed: 8978693]

Schuck S, Stenlund A. Assembly of a double hexameric helicase. Mol Cell 2005;20:377–389. [PubMed: 16285920]

Seki T, Diffley JF. Stepwise assembly of initiation proteins at budding yeast replication origins in vitro. Proc Natl Acad Sci U S A 2000;97:14115–14120. [PubMed: 11121019]

Shechter DF, Ying CY, Gautier J. The intrinsic DNA helicase activity of Methanobacterium thermoautotrophicum delta H minichromosome maintenance protein. J Biol Chem 2000;275:15049–15059. [PubMed: 10747908]

Sheu YJ, Stillman B. Cdc7-Dbf4 phosphorylates MCM proteins via a docking site-mediated mechanism to promote S phase progression. Mol Cell 2006;24:101–113. [PubMed: 17018296]

Takahashi TS, Wigley DB, Walter JC. Pumps, paradoxes and ploughshares: mechanism of the Mcm2-7 DNA helicase. Trends Biochem Sci 2005;30:437–444. [PubMed: 16002295]

Takeda DY, Shibata Y, Parvin JD, Dutta A. Recruitment of ORC or CDC6 to DNA is sufficient to create an artificial origin of replication in mammalian cells. Genes Dev 2005;19:2827–2836. [PubMed: 16322558]

Tanaka S, Diffley JF. Interdependent nuclear accumulation of budding yeast Cdt1 and Mcm2-7 during G1 phase. Nat Cell Biol 2002;4:198–207. [PubMed: 11836525]

Tanaka S, Umemori T, Hirai K, Muramatsu S, Kamimura Y, Araki H. CDK-dependent phosphorylation of Sld2 and Sld3 initiates DNA replication in budding yeast. Nature 2007;445:328–332. [PubMed: 17167415]

Tatsumi Y, Ezura K, Yoshida K, Yugawa T, Narisawa-Saito M, Kiyono T, Ohta S, Obuse C, Fujita M. Involvement of human ORC and TRF2 in pre-replication complex assembly at telomeres. Genes Cells 2008;13:1045–1059. [PubMed: 18761675]

Tsaneva IR, Muller B, West SC. RuvA and RuvB proteins of Escherichia coli exhibit DNA helicase activity in vitro. Proc Natl Acad Sci U S A 1993;90:1315–1319. [PubMed: 8433990]

VanLoock MS, Alexandrov A, Yu X, Cozzarelli NR, Egelman EH. SV40 large T antigen hexamer structure: domain organization and DNA-induced conformational changes. Curr Biol 2002;12:472–476. [PubMed: 11909532]

Weinreich M, Liang C, Stillman B. The Cdc6p nucleotide-binding motif is required for loading mcm proteins onto chromatin. Proc Natl Acad Sci U S A 1999;96:441–446. [PubMed: 9892652]

Wessel R, Schweizer J, Stahl H. Simian virus 40 T-antigen DNA helicase is a hexamer which forms a binary complex during bidirectional unwinding from the viral origin of DNA replication. J Virol 1992;66:804–815. [PubMed: 1309914]

West SC. Molecular views of recombination proteins and their control. Nat Rev Mol Cell Biol 2003;4:435–445. [PubMed: 12778123]

Wigley DB. ORC proteins: marking the start. Curr Opin Struct Biol 2009;19:72–78. [PubMed: 19217277]

Wilmes GM, Bell SP. The B2 element of the Saccharomyces cerevisiae ARS1 origin of replication requires specific sequences to facilitate pre-RC formation. Proc Natl Acad Sci U S A 2002;99:101–106. [PubMed: 11756674]

Woodward AM, Gohler T, Luciani MG, Oehlmann M, Ge X, Gartner A, Jackson DA, Blow JJ. Excess Mcm2-7 license dormant origins of replication that can be used under conditions of replicative stress. J Cell Biol 2006;173:673–683. [PubMed: 16754955]

Wyrick JJ, Aparicio JG, Chen T, Barnett JD, Jennings EG, Young RA, Bell SP, Aparicio OM. Genome-wide distribution of ORC and MCM proteins in S. cerevisiae: high-resolution mapping of replication origins. Science 2001;294:2357–2360. [PubMed: 11743203]

Zegerman P, Diffley JF. Phosphorylation of Sld2 and Sld3 by cyclin-dependent kinases promotes DNA replication in budding yeast. Nature 2007;445:281–285. [PubMed: 17167417]

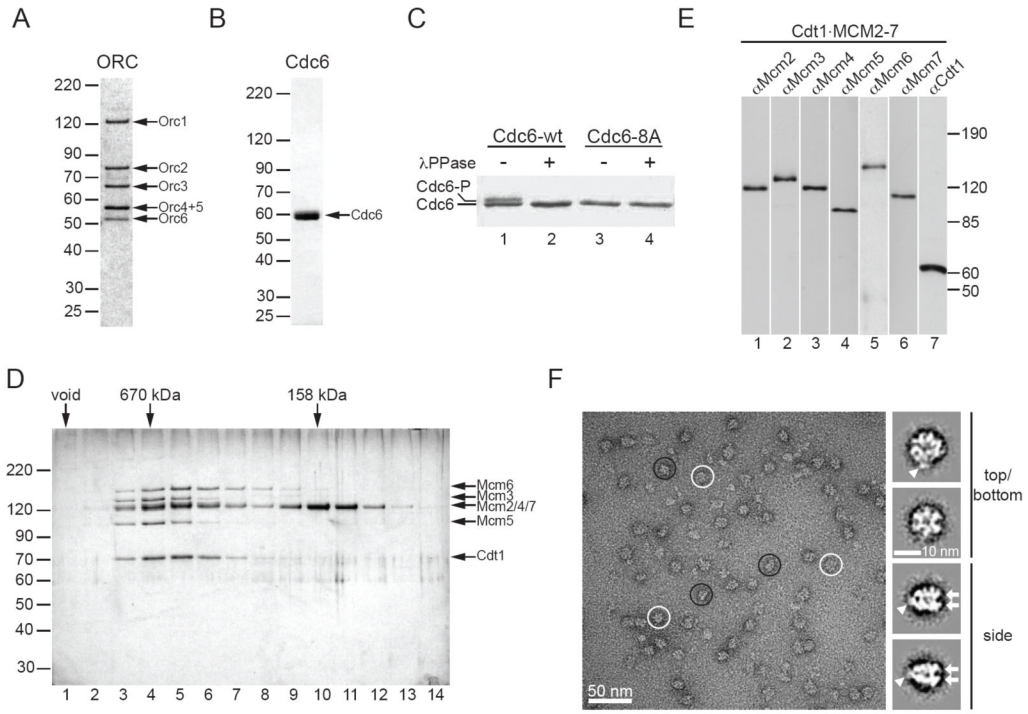

Figure 1. Purification of pre-RC proteins

(A and B) Purified ORC and Cdc6, respectively, analyzed by SDS-PAGE and Coomassie staining of the gel. Molecular mass markers (kDa) are indicated on the left, positions of ORC and Cdc6 are indicated on the right, respectively.

(C) Purified Cdc6-wt (lanes 1-2) and Cdc6-8A (lanes 3-4) were analyzed by SDS-PAGE and Coomassie staining before (lanes 1 and 3) and after (lanes 2 and 4) λ-phosphatase treatment.

(D) Gel-filtration analysis of Mcm4-FLAG immuno-affinity purified from whole-cell extract. Fractions were analyzed by SDS-PAGE and silver staining. Elution positions of molecular size markers (thyroglobulin, 670 kDa; bovine γ-globulin, 158 kDa) and the void position are indicated on the top. Gel-positions of identified proteins are indicated on the right.

(E) Western blot analysis of purified Cdt1·Mcm2-7 complex using specific antibodies indicated on the top of each lane.

(F) Transmission electron microscopy of negatively stained purified Cdt1·Mcm2-7. A representative micrograph is shown on the left. Examples of side-views and top-views are encircled in black and white, respectively. Panels on the right show representative reference-free class averages of top/bottom (upper two panels) or side views (lower two panels). The class averages, resulting from 4 rounds of SPIDER alignment and IMAGIC classification, corresponds to 65, 47, 58 and 55 aligned images, respectively (top to bottom). Arrowheads indicate an asymmetric protein appendage. Arrows indicate the two stacked protein layers in the side view.

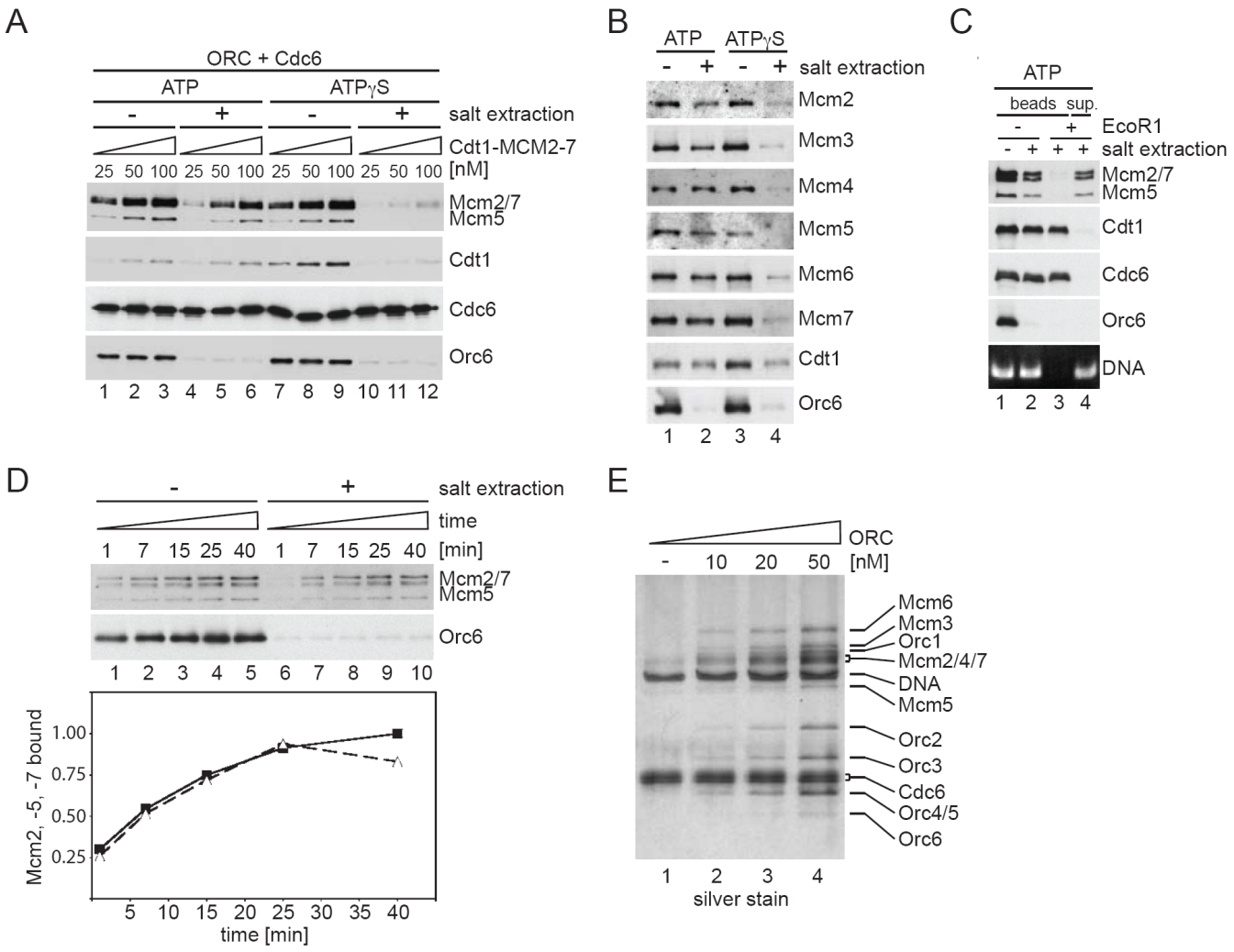

Figure 2. Reconstitution of Mcm2-7 loading *in vitro*

(A) Western blot analysis of DNA-bead-bound fractions of loading reactions performed at a constant concentration of ORC (25 nM) and Cdc6 (50 nM) and indicated concentrations of Cdt1·Mcm2-7. Reactions were performed in presence of 5 mM ATP (lanes 1-6) or 5 mM ATPγS (lanes 7-12). Beads were washed twice with low-salt buffer (0.3 M K-glutamate; lanes 1-3 and 7-9) or once with low-salt and once with high-salt (0.5 M NaCl) buffer (lanes 4-6 and 10-12). Proteins analyzed are indicated on the right.

(B) DNA bead association of all six MCM subunits (Mcm2-7) and indicated proteins following loading reactions in the presence of ATP (lanes 1-2) or ATPγS (lanes 3-4) without (lanes 1 and 3) and with (lanes 2 and 4) high-salt extraction.

(C) Loading was performed in the presence of ATP and DNA-bead association of the indicated proteins after low-salt (lane 1) or high-salt wash (lane 2) was analyzed by Western blotting. High-salt-washed beads of a loading reaction in ATP were subjected to EcoR1 cleavage and proteins present in the bead-containing (lane 3) or supernatant DNA-containing (lane 4) fraction were analyzed. DNA was analyzed by 0.8% agarose gel electrophoresis and ethidium bromide staining (bottom panel).

(D) Time course analysis of Mcm2-7 loading. ORC and Mcm2-7 binding to DNA-beads was monitored at the indicated time points after low-salt (lanes 1-5) or high-salt (lanes 6-10) wash. Quantified Western blot signals for Mcm2, -7, and -5 at the indicated time points after low-

salt (closed squares) or high-salt (open triangles) wash are plotted in the bottom graph relative to loading at 40 min after low-salt wash.

(E) Silver-stained SDS-PAGE gel analysis of loading reactions performed in the presence of 50 nM Cdc6, 50 nM Cdt1·Mcm2-7, and increasing amounts of ORC as indicated. Visible bands are annotated on the right.

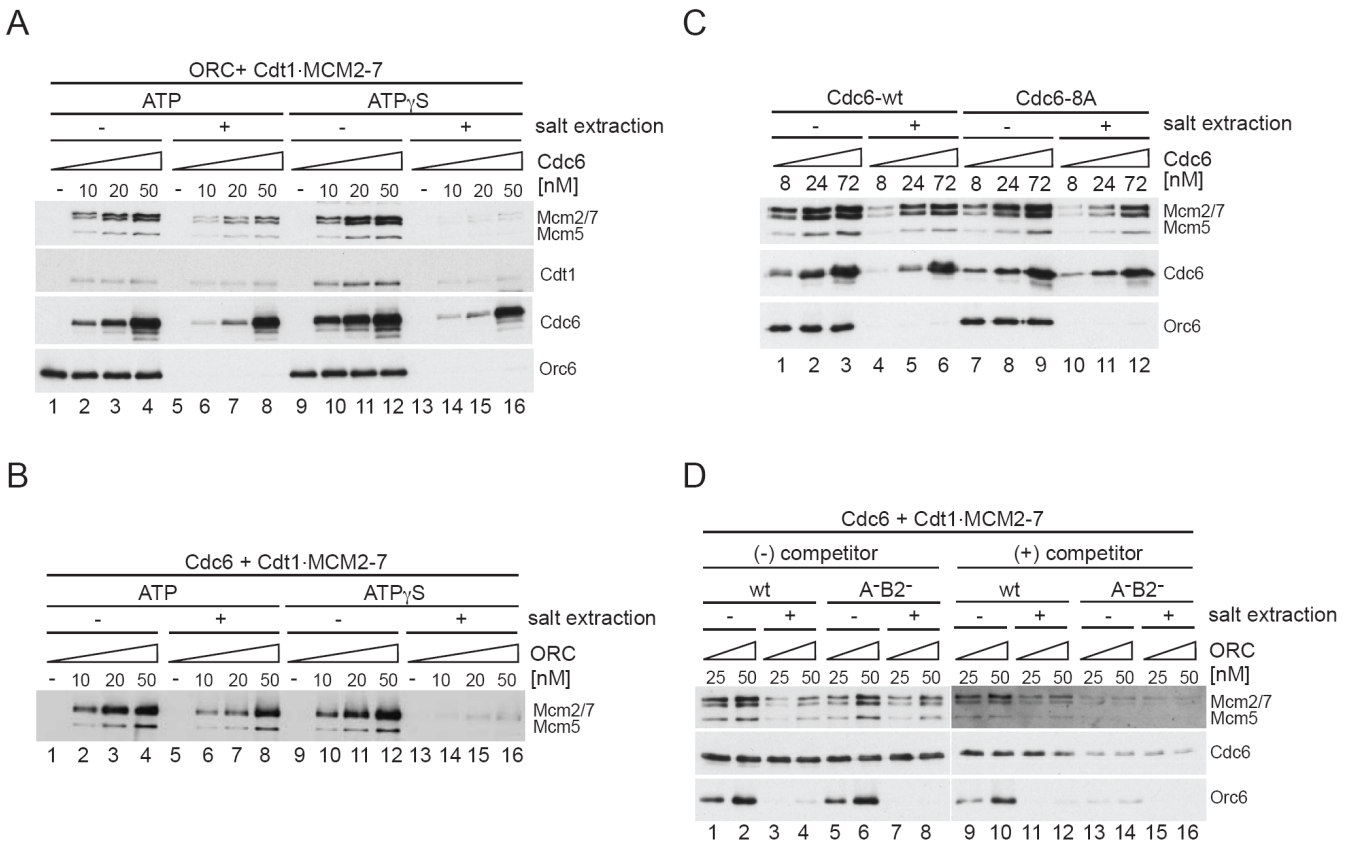

Figure 3. Protein and DNA sequence dependencies of Mcm2-7 loading *in vitro*

(A) Loading reactions performed in the absence (lanes 1, 5, 9, and 13) or presence of indicated amounts of Cdc6 (lanes 2-4, 6-8, 10-12, 14-16. All reactions contained ORC (25 nM) and Cdt1·Mcm2-7 (50 nM) and either 5 mM ATP (lanes 1-8) or 5 mM ATPγS (lanes 9-16).

(B) Loading reactions carried out in the absence or presence of indicated amounts of ORC. All reactions contained Cdc6 (50 nM) and Cdt1·Mcm2-7 (50 nM) and either 5 mM ATP (lanes 1-8) or 5 mM ATPγS (lanes 9-16).

(C) Comparison of the loading efficiencies of wild-type Cdc6 (lanes 1-6) and Cdc6-8A (lanes 7-12). Reactions were performed in the presence of 5 mM ATP, 25 nM ORC, and 50 nM Cdt1·Mcm2-7, and Cdc6 protein as indicated.

(D) DNA sequence specificity of Mcm2-7 loading in vitro. Reactions contained 50 nM Cdc6, 50 nM Cdt1·Mcm2-7, 5 mM ATP, and either 25 nM or 50 nM ORC as indicated. Binding to wild-type ARS1 DNA (lanes 1-4 and 9-12) or A$^-$B2$^-$ mutant ARS1 (lanes 5-8 and 13-16) was monitored either in the absence (lanes 1-8) or presence (lanes 9-16) of 0.8 mg/ml poly(dIdC)·poly(dIdC) and 10 mg/ml BSA.

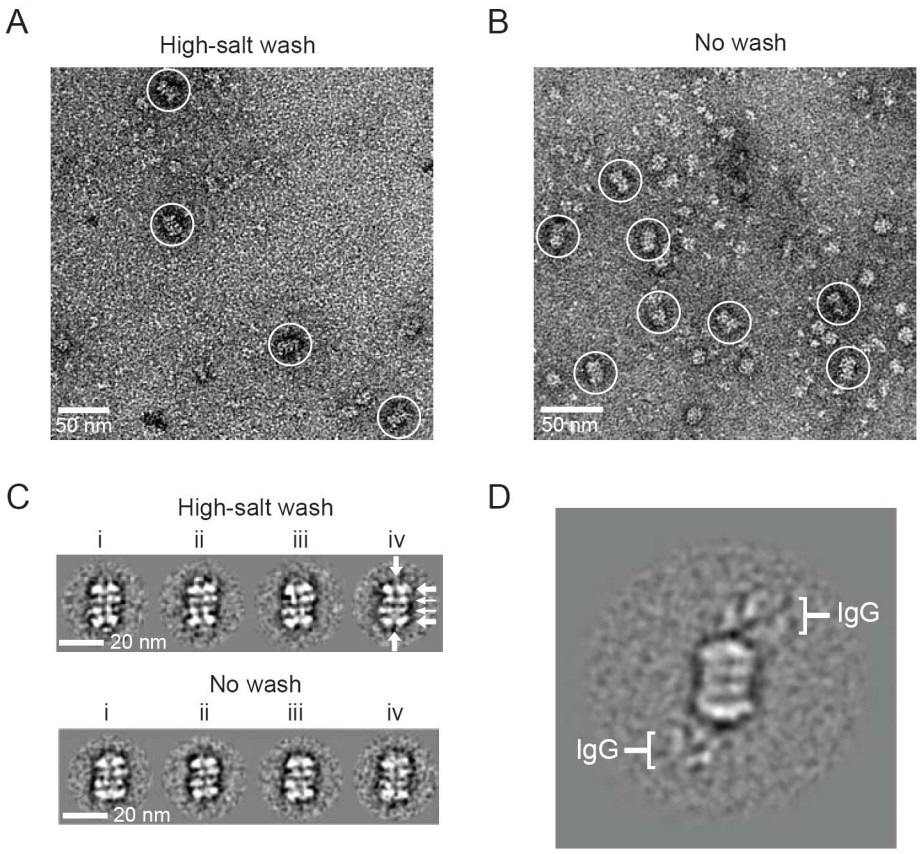

Figure 4. Transmission electron microscopy of negatively stained Mcm2-7 double hexamers

(A) Representative micrograph of DNA-bound Mcm2-7 complexes eluted from bDNA beads after high-salt-wash fraction by EcoR1 cleavage. Rectangular, four-tiered Mcm2-7 double hexamers are encircled.

(B) Micrograph showing proteins of complete loading reaction performed in solution. Mcm2-7 double hexamers (encircled) are distinguishable among other particles corresponding to free Cdt1·Mcm2-7, ORC and Cdc6.

(C) Representative class averages (i-iv) of Mcm2-7 double hexamers containing ~100 particles each. Averages in the top row were obtained from purified particles as in (A), averages in the bottom row were obtained from particles observed in whole loading reactions as in (B). Horizontal arrows mark the four tiers of the Mcm2-7 double hexamer side view; thicker arrows mark the AAA+ containing outer tiers, thinner arrows mark the inner N-terminal tiers. Vertical arrows indicate the path of the central channel.

(D) Class average of ~100 particles of Mcm2-7 double hexamers bound to α-FLAG IgG directed against the Mcm4 C-terminus. Brackets mark extra density due to bound IgG.

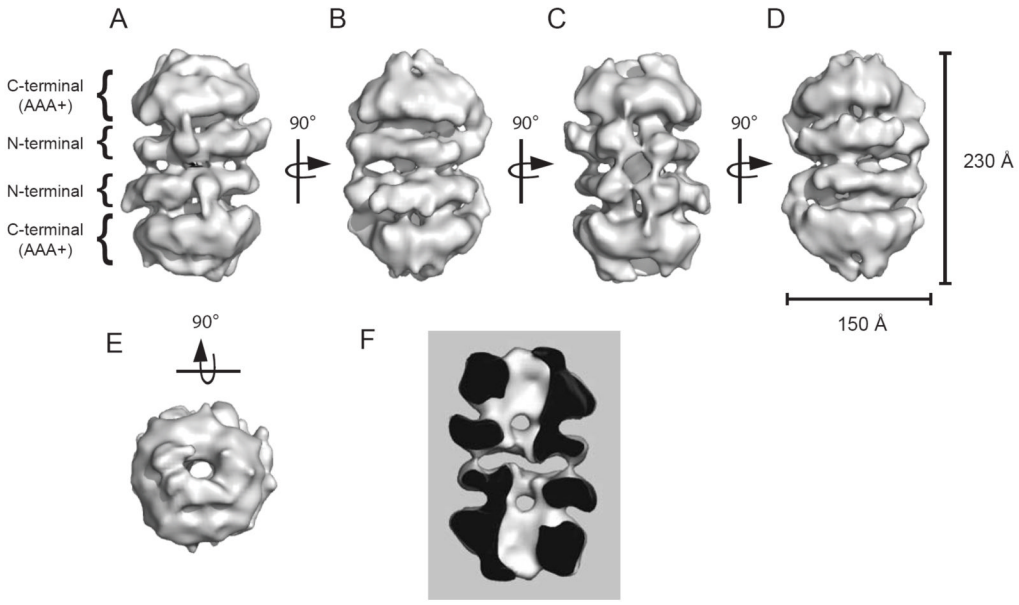

Figure 5. 3D reconstruction of the Mcm2-7 double hexamer

(A-E) Surface representations of a 3D reconstruction of the Mcm2-7 double hexamer filtered to 30 Å at the predicted molecular weight for the Mcm2-7 double hexamer. (F) Cut-open side view. Channel dimensions at various positions are indicated.

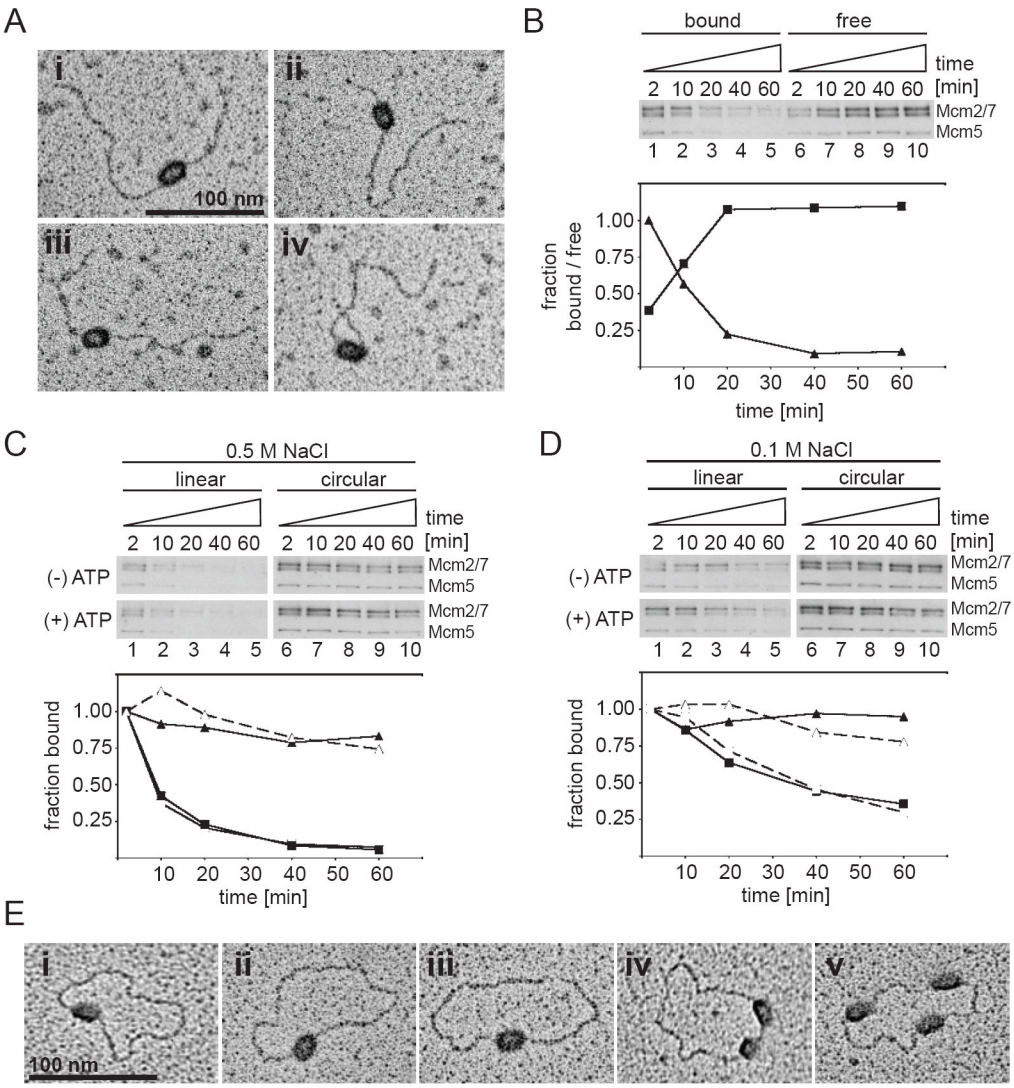

Figure 6. Mcm2-7 double hexamers can slide on DNA

(A) Mcm2-7 double hexamers bound to linear 1kb ARS305-containing DNA visualized after tungsten rotary shadowcasting.

(B) Time course analysis of Mcm2-7 retention on linear DNA after loading. Following the final high-salt wash of a loading reaction DNA beads were resuspended in 25 mM Hepes-KOH pH 7.6/0.5 M NaCl/5 mM $Mg(OAc)_2$/0.02% NP-40/10% glycerol/1 mM DTT. The suspension was incubated at 30°C and at the indicated time points an aliquot was removed from the suspension and DNA-bead-associated fractions (lanes 1-5) and supernatant fractions (lanes 6-10) analyzed by Western blotting. Quantified Western blot signals are plotted in the graph below (squares: supernatant; triangles: DNA-bead-associated).

(C) Time-dependent Mcm2-7 double hexamer retention on linear (lanes 1-5) or circular (lanes 6-10) 1 kb ARS305 DNA. DNA beads after a loading reaction were resuspended in buffer as in (B) either in the absence (upper panels) or presence of 5 mM ATP (lower panels). MCM2, -7, and -5 Western blot signals in each time course experiment were quantified, normalized in each series to the earliest time point, and plotted in the graph below (closed triangles, circular DNA (-) ATP; open triangles, circular DNA (+) ATP; closed squares, linear DNA (-) ATP; open squares, linear DNA (+) ATP).

(D) As (C), except that Mcm2-7 retention on DNA was monitored in buffer containing 0.1 M NaCl instead of 0.5 M NaCl.
(E) Mcm2-7 double hexamers bound to circular 1kb ARS305-containing DNA visualized as in (A).